Miloš Jelić
Research Associate
Yugoslav Accreditation Council, Belgrade

Mitar Mišović
Professor

Nebojša Tadić
Research Associate

Faculty of Metallurgy and Technology, Podgorica

A Method for Determination of Axial Residual Stresses in Drawn Bars

The paper describes a genuine deflection method based on correlation between non-homogenous yielding and residual stresses, obtained by monitoring of "attached sample halves" balance. Results obtained by this method enabled generation of (square parabola) elastic line equation. Estimated error justifies the implementation of linear stress distribution over cross-section in testing range 330 – 550 MPa.

Keywords: *Residual stresses, drawn bar, attached sample halves*

1. INTRODUCTION

Metal products manufacturing is often characterized by non-homogenous processes, which are permanently accumulated in the material producing residual macro and micro stresses. Macro stresses are balanced in volume and they may be considered as a tensor that represents space or plane stress state. If the stresses are generated by strain, their tensor components are determined by material flow. Cold drawing process in bars typically generates radial (σ_r), axial (σ_z) and hoop (σ_θ) stresses [1-4].

Residual stresses, generated by drawing process, are the consequence of non-homogenous flow due to shape of deformation zone and contact phenomena at the interface. Typically, when bars are concerned, residual stresses caused by cooling after hot rolling may become significant. Thus, a simple and reliable evaluation of residual stresses in bars is important for their safe service life. Of special concern is the axial component of residual stresses.

In this paper the experimental method using attached specimen halves has been used to evaluate axial residual stress distribution in drawn bars.

2. EXPERIMENTAL PROCEDURE

2.1. Sample preparation

The two sample halves are joined in appropriate way and submitted to drawing. Samples were drawn on a production drawing machine. By detaching two halves, sample shape as shown in Fig. 1*a* is obtained. Samples have to be long enough to provide lag determination according to Peiter's formula, $l/D>10$ [5], where l is bar length and D bar diameter.

After detaching the distances between two halves at different z positions are measured. Test scheme with sample bar dimensions and basic drawning data is presented in Table 1. Three different steels were used, also defined in Table 1.

Received: February 2002, revised: February 2004, accepted: April 2004.

Correspondence to: Miloš Jelić
JUAT, Bulevar Mihajla Pupina 2a, 11070 Belgrade, SCG
E-mail: milosj@gov.yu

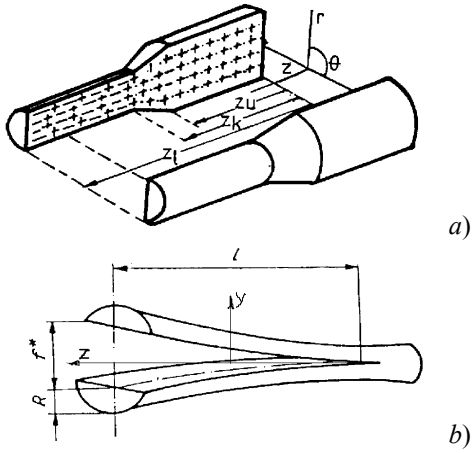

Fig. 1. Samples for residual stress determination

2.2. Results and analysis

Measured distances between two bar halves in $(0,l)$ range for sample 2.1 are shown in Table 2. Due to symmetry, elastic line for one sample half equals to the half of distances.

Detaching of "attached" samples may be linked with disruption of axial residual stress balance. Bending of sample halves may be considered as bar having constraint in undetached state. Since stress distribution in cross-section remains constant lengthwise bending moment appears to be constant, as well. Therefore, elastic line equation may be presented as follows:

$$y = f^*(z/l)^2, \tag{1}$$

where f^* denotes the maximum deflection, and z/l the relative distance from the undetached bar end.

Verification of equation (1) is done through comparison with test results, as shown in Fig. 2. Although differences are relatively small they are still significant. Therefore, test results are fitted also by the following equation:

$$y = c_1 z/l + f^*(z/l)^2 \tag{2}$$

Results obtained by using Eqn. (2) are plotted in Fig. 2. High correlation of results with the entire elastic line indicates that the approximation error falls below test

Table 1. Axial residual stress testing scheme

Material	Sample No	Input Diameter (mm)	Output Diameter (mm)	Drawing conditions		
				Speed (m/s)	Lubricant	Die angle (rad)
Steel 1 (0.2% C, 1.3% Mn, 0.32% S)	1.1	21.2	20.2	0.35	Oil	0.314
	1.2	17.9	16.1	0.35	Oil	0.314
Steel 2 (0.12 – 0.18% C) E = 191.4 GPa	2.1	16	15	0.35	Oil	0.314
	2.2 2.3		14.5			
Steel 3 (0.18% C, 0.8% Cr) E = 210.9 GPa	3.1 3.2	32	30	0.35	Paste	0.314

Table 2. Measured distances between meridian surfaces with sample 2.1

Position	0	25	50	75	100	125	150	175	200	225	250
Deflection	0	0,80	2,00	3,64	5,80	8,40	11,40	14,84	18,90	23,40	-

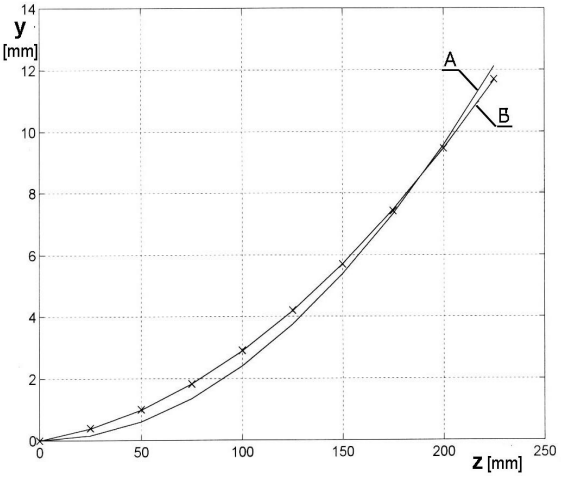

SAMPLE - 1 drawn
x - test result

A - calculated according to: $y = a_1 z_n^2$

B - calculated according to: $y = a_2 z_n + a_3 z_n^2$

Elastic line equation	MSE	d^2y/dz^2
$y = 14,96\ z_n^2$	0,62	$4,79 \cdot 10^{-4}$
$y = 2,62\ z_n + 11,49\ z_n^2$	0,01	$3,68 \cdot 10^{-4}$

Fig. 2 - Comparison of results for elastic line

error. It may be noted that scatter of results obtained by Eqn. (1) is more significant near z=0 position where influence of linear term appears to be rather strong. More thorough analysis shows that departures are not caused by inappropriate approximation model but the reason may be found in imperfect joint. It may be assumed that the joint gets loose after drawing thus changing elastic line in the vicinity of the of the joint [6]. Therefore, in following calculation both equation will be applied in further considerations.

3. BALANCE AFTER DEFLECTION

Moment causes elastic bending of detached sample halves after detaching samples at one end. Since stress values appear to be constant lengthwise the bending moment arising after balance disruption remains constant, as well. General relation for bar bending subject to constant moment is:

$$E I_x \frac{1}{\rho} = |M_s|,$$

where:
E - Young modulus,
I_x - Moment of inertia for bending axis,
ρ - Curvature radius of elastic line.

If M_s=const. lengthwise and assuming elastic line inclination significantly less than 1, one gets

$$M_s = \frac{2 E I_x f^*}{l^2},$$

where f^* represents deflection rate at joint free bar end.

To link residual stresses and bending state for detached barit is necessary to determine relation for moment arising from internal stress balance disruption. Taking into account the facts that residual stresses have constant value in z direction and the axial symmetry in θ direction, their distribution reduces to R direction. Axial symmetry also simplifies space distribution of residual stresses enabling changeover to equivalent external moment or parallel equal counter-directed forces exerting on barelement (Fig. 3).

The analysis starts from the balance of the bending moment and moment induced by residual stresses. Assuming linear distribution of residual stresses over radius R, 'zero stress' radius is located at $2/3R_o$, where R_o is the outer raduus. The following relations may be obtained:

$$F = \frac{4}{27}\pi R_o^2 \sigma_p \quad ; \quad l = \frac{8}{9\pi} R_o \quad ;$$

$$M_s = \frac{2}{12} R_o^3 \sigma_p = \frac{2 E I f}{l^2}$$

and in turn:

$$\sigma_p = 12\left(\frac{\pi}{8} - \frac{8}{9\pi}\right)\frac{R_o E f}{l^2},$$

with σ_p denoting residual stress at the surface.

From Fig. 3*b* it comes out:

$$m = \frac{3\sigma_p I_{KI}}{2R_o}$$

with I_{KI} denoting inertia moment of $R_0 d\varphi$, leading to the same expression for σ_p.

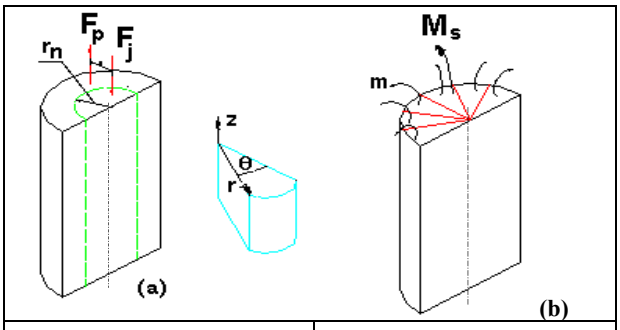

Force in ring:

$$F_p = 2\int_0^{\pi/2}\int_{r_n}^{R_o} \sigma(r)\,dA$$

Force in ring:

$$F_p = 2\int_0^{\pi/2}\int_0^{r_n} \sigma(r)\,dA$$

$$F_p = F_j = F$$

Ring mass center:

$$X_p = \frac{1}{F_p}\int_A X_C\,dA$$

Core mass center:

$$X_j = \frac{1}{F_j}\int_A X_c\,dA$$

Mass centers distance:

$$l = X_p - X_j$$

Bending moment:

$$M_s = F\,l$$

Overall moment:

$$M_s = 2\int_0^{\pi/2} m\sin\varphi\,R_o d\varphi\,,$$

where m - denotes moment of $R_0 d\varphi$ element constraint free from adjacent elements in θ-direction

$$M_s = 2\,m\,R_o$$

Figure 3. Changeover from residual stress effects to external stress load: a – constraint substitution like in experiment; b – for residual stress removal.

Linear distribution model, being the initial assumption, determines residual stress value at each *r*-location. Coefficients in the linear model may be reckoned out of the stress balance in the entire sample half. Another possibility is to accume the parabola of n-th order as a more general solution:

$$\sigma_z = \sigma_p\,(C\,r_n^n + B)$$

with σ_z denoting axial component of residual stresses, σ_p axial component of residual stresses at the surface, $r_n = R/R_0$ relative radius.

At bar surface:

$$r_n = 1\,,\quad \sigma_z = \sigma_p\,,\quad C + B = 1\;;$$

and balance condition in overall volume:

$$\int_0^{\pi}\int_0^1 \sigma_p\,(C\,r_n + B)\,r_n\,dr_n\,d\varphi = 0\,.$$

General solutions for coefficients enable equation formation, i.e. general distribution model for axial residual stress as a function of bardiameter:

$$\sigma_z = \sigma_p\left[(1+\frac{2}{n})\,r_n^n - \frac{2}{n}\right]$$

Particular solutions up to parabola of fourth order show axial stress decrease ranging from $-2\sigma_p$ (linear distribution) up to $-0{,}5\sigma_p$ (fourth order parabola) while σ_p remains constant. Resulting force (F) at the same time decreases 1,54 times along with mass center distances thus resulting in moment decrease of 1,75 times.

If moment is considered constant, its value depends upon the order of parabola

$$M_s = \frac{2}{3(3+n)}R_o^3\,\sigma_p\,,$$

leading to the equation for surface residual stress:

$$\sigma_p = \frac{9\pi^2 - 64}{24\pi}(3+n)\,R_o\,E\,\frac{f}{l^2} \qquad (3)$$

This equation shows that surface residual stress has the increment of 25% for each increase of parabola order if moment is kept constant.

3.1. Axial residual stress values in drawn bars

Stresses at barsurface, which have been calculated for sample 2.1 using linear distribution model (n=1), are shown in Fig. 4. Rather strong influence of linear term in Eq. (2) caused high stress values in the vicinity of rivet joint and their reduction lengthwise. Unlike that, stresses obtained from Eq. (1) remain constant lengthwise due to constant bending moment. It should be observed that stresses obtained by these two models become practically equal at the joint free end.

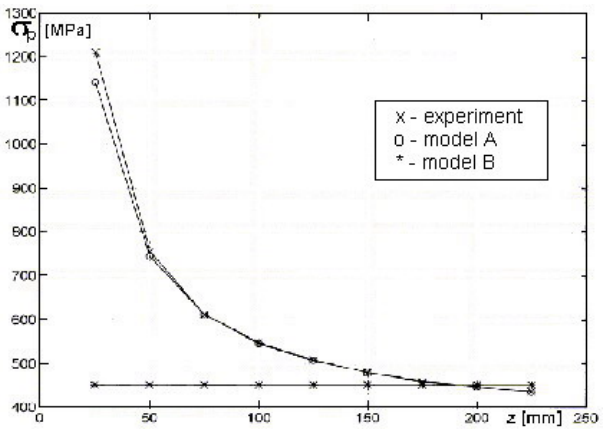

Fig. 4. Calculated surface stress values along sample 2.1 (x–experimental, o–model A, *-model B)

The scatter of calculated values is caused by errors made in deflection measurements, i.e. elastic line approximations. If the error is defined as mean square

error in relation to measured values, differences between measured values and values obtained by Eq. (2) become virtually negligible. Unlike that, the approximation error generated by Eq. (1) is larger, thus producing rather significant result dissipation. However, even in that case mean square error at the joint free barend falls beneath errors made in measurements. This conclusion provides confidence in obtained values and at the same time confirms the applicability of the method used if bar length is significantly higher than bardiameter. The experiments carried out [6] indicate that length to diameter ratio should be:

$\frac{l}{R_o} \geq 12$ - with sample diameter 15 mm and

$\frac{l}{R_o} \geq 10$ - with sample diameters 30 and 40 mm.

By using these criteria, stresses are calculated for deflection values at z=225 mm in the latter case. Calculated values are given in Table 3.

Table 3. Surface residual stress values calculated for z=225 mm

SAMPLE	Elastic line equation	STRESS (MPa) z=225 mm
		Linear distribution
1.2	Experiment	432,8
	Model A	432,6
	Model B	432,1
2.1	Experiment	338,1
	Model A	338,7
	Model B	337,6
3.2	Experiment	564,4
	Model A	571,1
	Model B	523,9

4. CONCLUSIONS

Calculated surface stress values depend on accuracy of all terms in Eq. (3). Bardiameter after calibration drawing may be determined with high accuracy. The same applies to Young modulus and to elastic line determination. So, the major impact remains on stress distribution model. A quite reliable approximation is obtained when Eq. (2) is used. Deflection values from experiments that depart from Eq. (1) values within measurement error may be used for stress calculations only. Therefore, no matter initial differences due to linear term are present (arising from curve radius equation $1/\rho = y''/(\sqrt{1+y'})^3$; they may be disregarded if defined criteria for length-to-diameter ratio are respected in deflection measurements.

Since above experiments undoubtedly justify the application of stress linear distribution model over cross section it may be concluded that axial residual stresses for test program given in Table 3 are in the range 330–550 MPa.

REFERENCES

[1] Williems F.P., Naughton P.B., Mater. Sci. and Techn., 1, pp. 41-44, 1985.

[2] Bonner W.N., Residual Stresses in Multi-pass Cold Drawing of High Carbon Steel Wire, Proc. of ECRS-4, Cluny, pp. 755-765, 1996.

[3] Hartley S.C., Dehghani M., Residual stresses in axi-symmetrically formed products, "Advanced Technology of Plasticity", Vol I, pp. 605-611, 1986.

[4] Coppola T. et al., Evaluation of Stresses in Cold Drawn Tubes, Proc. of ECRS-4, Cluny, pp. 475-485, 1996.

[5] Peiter A., *Handbuch Spannungs Messpaxis*, Wieweg, pp. 98-108, 1992.

[6] Jelic M., Ph. D. thesis, *The investigation of residual stresses in final production processes and the importance of their distribution models on metal properties selection*. Metalursko-tehnoloski fakultet, Podgorica, 1998.

МЕТОДА ОДРЕЂИВАЊА АКСИЈАЛНИХ ЗАОСТАЛИХ НАПОНА У ВУЧЕНИМ ШИПКАМА

Милош Јелић, Митар Мишовић, Небојша Тадић

У раду је описана оригинална метода дефлекције, која је заснована на корелацији нехомогеног течења и заосталих напона, добијеној прецизним праћењем равнотеже »састављених половина узорака«. Резултати добијени применом ове методе омогућили су извођење једначине еластичне линије (облика квадратне параболе). Процењена грешка оправдава примену линеарног модела расподеле заосталог напона по попречном пресеку за програм испитивања у опсегу 330 до 550 MPa.